Nordic Hydrology, 34 (3), 2003, 179-202
No part may be reproduced by any process without complete reference

Seasonal Water Balance of an Alpine Catchment as Evaluated by Different Methods for Spatially Distributed Snowmelt Modelling

M. Zappa[1], F. Pos[2], U. Strasser[3], P. Warmerdam[2] and J. Gurtz[1]

The application of three temperature-index based models and of one energy balance based snowmelt model was investigated. The snow models were integrated in the spatially distributed hydrological model PREVAH. In this study the hydrological simulations of the alpine catchment of the Dischmabach in Switzerland in the period 1982-2000 have been analyzed. The PREVAH model was driven by hourly interpolated meteorological data.

All snowmelt approaches allowed a good simulation of the discharge regime and of the seasonal course of the snowpack. The highest model efficiency was obtained by a radiation based temperature-index approach. A simplified energy balance approach combined with the positive degree-day method showed a very similar performance to the classical positive degree-day approach. The energy balance approach ESCIMO showed a high performance variability from year to year.

The dependency of the seasonal water balance with respect to altitude is also discussed in this report. The quality of the spatially distributed reproduction of periods with positive and negative water balance (snow accumulation and snowmelt) is crucial for the correct simulation of the runoff hydrograph. The analysis shows that runoff maximum in the Dischmabach catchment is caused by a superposition of the main snowmelt season in the areas between 2,100-2,800 m a.s.l. and the period with maximum rainfall.

[1]Institute for Atmospheric and Climate Science, ETH, Zürich
[2]Dept. of Environmental Sciences, Wageningen University
[3]Inst. of Hydromechanics and Water Resources Mgm. ETH, Zürich

Introduction

The choice for temperature-index or energy balance based approaches for the computation of the snowmelt processes is a subject of frequent discussions in the scientific community dealing with snow hydrology and glaciology (WMO 1986; Ferguson 1999). The topical discussion includes the dilemma of using conceptual (Braun *et al.* 1994) or physically-based models (Abbot *et al.* 1986; Beven 1989), the importance of the model structure (Braun *et al.* 1994; Klok *et al.* 2001) and scaling issues (Blöschl and Sivapalan 1995; Blöschl 1999).

Klemeš (1990) discusses the differences between conceptual and physically-based snowmelt models with respect to their structure, need of data and calibration requirements. The more free parameters are available to fit the model for a selected catchment, the more it is possible to compensate the cumulative error caused by:

- observation of the target variables (discharge and snow water equivalents)
- parameterization (soil, physiographic and vegetation-specific parameters)
- conceptual representation of the hydrological processes (*e.g.*, assumption of the linear response of storage reservoirs, separation between snow and rain, correction of precipitation)
- meteorological input data (plot-scale and/or interpolated).

Physically-based models, such as energy balance based snow models, tend to increase the *a priori* parameterization of the processes and to reduce the need of calibration to a minimum number of free parameters. This allows the transfer of experience from one catchment to another without starting the calibration again from scratch. The disadvantage is that an increased number of variables needs to be observed. Detailed snowmelt routines based on the parameterization of the energy balance are often integrated in land surface schemes (LSS). LSS have been the target of several studies at plot-scale. Recent studies, focussing on the snowpack, have been published by Slater *et al.* (2001) and Essery *et al.* (1999).

Conceptual models, such as temperature-index based snow models (Lang and Braun 1990; Ohmura 2001), allow model application with fewer input variables. By tuning the free parameters the specifications of the catchment under investigation are captured. This generally increases the model performance within a catchment, but gives few indications for the transfer of the results to other regions. Measurement and spatial interpolation of air temperature with high resolution is easier to realize than detailed energy balance observations. Therefore, model users tend to apply temperature-index methods (Hock 2003) for spatially distributed hydrological simulations (Kirnbauer *et al.* 1994). Ohmura (2001) provides a thorough physically-based answer to the question why empirical temperature-based methods are effective, as generally shown in snow and ice melt computations. The temperature-index models perform that well, because the air temperature is a particularly representative diagnostic variable for the three major energy sources which determine snow and ice melt, namely incoming longwave radiation, absorbed global radiation and sensible heat flux.

Alpine catchments are extremely heterogeneous and therefore appropriate to assess the proposed topics. This heterogeneity is determined by the complexity of their physiography as well as by a large seasonal course of the climatic variables (Gurtz *et al.* 1999). The hydrological models should represent this heterogeneity to cope with the hydrological complexity of this particular environment, where the assessment of the spatial and temporal variations of snow is of crucial importance. This could also yield valuable information for an improved management of water resources in the alpine area.

This study investigates the modular implementation of three temperature-index snowmelt models and of the energy balance based snowmelt model ESCIMO (Strasser *et al.* 2002) as integrated in the hydrological model PREVAH (Gurtz *et al.* 1999). The target area is a Swiss alpine catchment with nival runoff regime. The different accuracy of the four approaches for the modelling of snow accumulation and melt is evaluated. The analysis also includes the discussion on the seasonal contribution of different elevation zones to the catchment discharge and on the role of topography in the spatial and temporal distribution of snowmelt.

Catchment

The *Dischmabach* catchment is located in the eastern part of Switzerland (Fig. 1), in the climatological transition zone between the wet northern Alps and the dry central Alps. The catchment area (gauge Kriegsmatten) is 43.3 km^2 and has a glacierized portion of 2.1% (Table 1). The elevation ranges from 1,668 to 3,146 m a.s.l. The river valley is oriented from south-south-east to north-north-west.

In the lower part of the catchment snowfall represents approximately 40% of the

Table 1 – Main characteristics of the Dischmabach catchment

Topography		Land use / soil cover:	
Catchment area (km^2)	43.3	Water areas	0.3
Mean altitude (m a.s.l.)	2378	Settlements	0.4
Gauge altitude (m a.s.l.)	1668	Pine forest	2.4
Highest point (m a.s.l.)	3146	Meadow	0.6
Mean slope (degrees)	24.6	Wet areas	0.1
		Bushes	7.1
Aspect classes:		Subalpine pastures	36.4
North (%)	24.0	Alpine meadows	1.3
East (%)	30.2	Gravel, pit / bare soil	15.8
South (%)	6.6	Rock	33.5
West (%)	39.0	Glacier	2.1

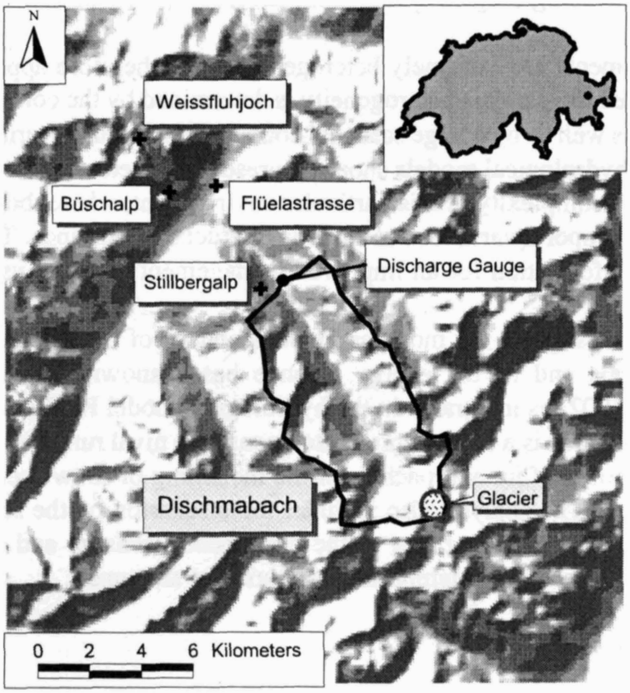

Fig. 1. Location of four stations (crosses) for the observation of the snow water equivalent, of the discharge gauge and location of the Dischmabach catchment within the map of Switzerland (point in the upper right box).

total precipitation, while in the highest elevation zone more than 80% of the total precipitation consists of snow. In the lower parts snow accumulates between November and February. In the higher parts of the catchment snow accumulation can be observed from November until the end of April (Fig. 3).

The only permanent hydrometeorological observations within the catchment are those of discharge and precipitation. However, at a few kilometers' distance, MeteoSwiss maintains the long-term fully equipped meteorological observatories of Davos (1,590 m a.s.l.) and Weissfluhjoch (2,690 m a.s.l.).

The Hydrological Model

The spatially distributed hydrological model *PREVAH (Precipitation-Runoff-Evapotranspiration-HRU model*, Gurtz *et al.* 1999) was used. The spatial discretization of PREVAH relies on the aggregation of units with similar hydrological response (HRU). The hydrological properties of the catchment are derived from gridded maps of elevation (BFLT 1991), land use, land cover and soil properties (BFS 1995). The assembling of the HRUs considered the elevation zones (15 classes), exposure (5 classes), land use (11 classes) and the equilibrium line altitude (ELA) of the glacier (Zappa *et al.* 2000). Thus 334 HRUs were generated for the Dischmabach catchment on the basis of 100x100m digital grids of the relevant physiographic characteristics.

The model subsystems are: a snow module, an interception module, a module for soil water storage and depletion by evapotranspiration (Monteith 1975), a glacier module (Klok *et al.* 2001) and a runoff generation module (Bergström 1976).

The model was run in an hourly time step. For each hour and elevation zone the average of interpolated values for precipitation (P), air temperature at 2 metres height (T_a), global radiation (G), wind speed (u), water vapor pressure (e_a) and relative sunshine duration (SSD) is required. The adopted interpolation procedure is a weighted combination of inverse distance weighting and altitude-dependent regression techniques (Schulla 1997; Klok *et al.* 2001). Temperature and radiation (either measured or potential) are locally adjusted with respect to aspect and slope of the HRUs. The procedure of assimilation of representative precipitation time series for the catchment under investigation includes the optimization of the parameters of the correction of rainfall and snowfall during the period of calibration. This is done to minimize differences between observed and computed runoff rates and to compensate for errors in the measurement and interpolation of precipitation (Sevruk 1986).

Snow Accumulation and Snowmelt

A separation between snow and rain is made to determine the snow accumulation. If the interpolated air temperature at 2 metres height T_a (°C) is lower than a calibrated threshold temperature T_{GR}, the phase of precipitation is solid. Otherwise the phase of precipitation is liquid. A transition parameter (T_{TRANS}) can be adopted to define the air temperature range where the phase of precipitation is considered a mixture of rain and snow. The snow fraction (p_{Snow}) is given by

$$p_{\mathrm{Snow}} = \frac{T_{GR} + T_{\mathrm{TRANS}} - T_a}{2\,T_{\mathrm{TRANS}}} \quad (T_{GR} - T_{\mathrm{TRANS}}) < T_a < (T_{GR} + T_{\mathrm{TRANS}}) \tag{1}$$

Four modular approaches for the snowmelt computation are available (Table 2):

1) Positive Degree-Day Index (PDDI): This basic temperature-index method requires only the availability interpolated temperature data. If T_a is below a threshold temperature for snowmelt (T_0) then the melt rate (M) is zero. If T_a exceeds T_0 then the melt rate is calculated according to

$$M = TMF_{PD}(T_a - T_o) \tag{2}$$

Table 2 – Data requirement and calibrated parameters of the snowmelt and runoff modules.

	Unit	PDDI	COMB	EMA	ESCIMO
SNOWMELT MODULE					
Required Input		T_a, P	T_a, P, e_a, u	T_a, P	T_a, P e_a, u, G, SSD
T_{GR}	[°C]	0.0	0.0	0.0	0.0
T_{TRANS}	[K]	0.5	0.5	0.5	
T_0	[°C]	-0.5	-0.5	-0.5	
$TMF_{PD\text{-}MIN}$	[m s^{-1} K^{-1}]	$2.8 \cdot 10^{-8}$	$2.2 \cdot 10^{-8}$		
$TMF_{PD\text{-}MAX}$	[m s^{-1} K^{-1}]	$5.8 \cdot 10^{-8}$	$5.8 \cdot 10^{-8}$		
c_1	[m s^{-1} K^{-1}]		$2.2 \cdot 10^{-8}$		
c_2	[K^{-1}]		$1.1 \cdot 10^{-8}$		
TMF_{EMA}	[m s^{-1} K^{-1}]			$9.3 \cdot 10^{-9}$	
RMF_{EMA}	[m^3 s^{-1} W^{-1} K^{-1}]			$7.5 \cdot 10^{-11}$	
ALB_{MAX}	[-]				0.90
A_{POS}	[h^{-1}]				0.07
A_{NEG}	[h^{-1}]				0.02
RUNOFF MODULE					
K_0	[h]	8	8	16	16
K_1	[h]	370	370	300	300
K_2	[h]	3200	3200	3200	3200
$PERC$	[mm h^{-1}]	0.09	0.09	0.09	0.09

The temperature dependent melt factor (TMF_{PD}) can be defined by a sinus shaped function of the threshold values between the annual maximum (set for June 21st) and minimum values (December 21st). In this differentiation, the seasonal variation of the solar radiation is taken into account (Braun 1985).

2) Combination approach (COMB): Anderson (1973) extended the PDDI method introducing a combination of radiation melt for dry periods and advection melt for wet days. Radiation melt occurs when the melt is dominated by radiation energy. This occurs when the precipitation is less than a threshold intensity. In that case snowmelt is calculated using Eq. (2). Advection melt occurs when rainfall exceeds a threshold intensity. In this case a simple empirical parameterization of the energy balance, Eqs. (3.a)-(3.e), is applied for the computation of snowmelt (Braun 1985). The total snowmelt M is the sum of the melt rates given by long wave radiation (M_R), sensible heat flux (M_S), latent heat flux (M_L) and precipitation (M_P)

$$M_R = f_R T_a \tag{3a}$$

$$M_S = (c_1 + c_2 u) T_a \tag{3b}$$

$$M_L = (c_1 + c_2 u)(e_a - 6.11)\gamma^{-1} \tag{3c}$$

$$M_P = f_p \, P \, T_a \tag{3d}$$

$$M = M_R + M_S + M_L + M_P \tag{3e}$$

f_R (1.4×10^{-8} m s^{-1} K^{-1}) and f_P (0.0125 K^{-1}) are parameterized constants; c_1 and c_2 are empirical model parameters (see Table 2) and γ is the psychrometer constant. COMB was first developed with the intent of improving the computation of snowmelt in lowland regions where heavy melting is often associated with rain-on-snow events (Braun 1985). Rain-on-snow events are seldom in the investigated high alpine Dischmabach basin, since most of precipitation falls in form of snow.

3) The extended melt approach (EMA): Hock (1999) proposed the extension of the temperature-index approach under consideration of the daily potential direct radiation variations

$$M = \begin{cases} (TMF_{EMA} + RMF_{EMA} \, I_0)(T_a - T_0) & T_a > T_0 \\ 0 & T_a \leq T_0 \end{cases} \tag{4}$$

I_0 is the site adjusted clear-sky direct solar radiation(corrected for slope and aspect), TMF_{EMA} is a temperature dependent and RMF_{EMA} a radiation dependent melt index. The inclusion of I_0 allows taking into account the pronounced daily cyclicity and the large spatial variability of the melt rates without increasing the required number of climate elements. The simulation of ice melt in the glaciated areas is also based on this approach (Hock 1999). A study focussed on the icemelt computation was presented by Klok *et al.* (2001).

4) The one-layer snow model ESCIMO (*Energy-Balance Snow Cover GIS-Integrated Model*) was developed for the hydrological simulation of the Weser catchment in Northern Germany (Strasser and Mauser 2001). It is designed as a physically-based model for the hourly simulation of the energy balance, the water equivalent and the melt rate of a snowpack. The principle and most influential terms of the energy balance are the short and longwave radiation, the sensible and latent heat fluxes. The energy conducted by solid or liquid precipitation and a constant soil heat flux are also taken into account for the energy balance computation, even if their contribution is rather limited. The snow albedo is modelled using a function considering the age and the surface temperature of the snowpack (Rohrer 1994). For each time step the following scheme is adopted (Abbott *et al.* 1986): calculation of the energy balance, decision whether the precipitation is solid or liquid, estimation of the water mass and energy budget based on the hypothesis of zero snowmelt at the current time step, comparison of the total available energy with

that sustained as snow by the total available mass at 273.16 K, calculation of the snowmelt produced by the available excess energy and a subsequent update of the mass and energy budgets. The number of free parameters is limited to the three. These control the simulation of the albedo (see Table 2), and are the maximal albedo (ALB_{MAX}) and the parameters determining the ageing of the albedo (A_{POS} for positive and A_{NEG} for negative snow temperature). The mathematical representations of the simulated physical processes as used in ESCIMO are described in Strasser *et al.* (2002).

Among the snowmelt modules used only ESCIMO tracks, without adjustments, the cold content of snowpack. To give a complete overview on the snowmelt modules it is to mention that the hydrological model allows, in case of the temperature-index modules, a parameterization of ripening within the snowpack and the use of a simple routing scheme to transfer liquid water through the snowpack. For this study it was decided to renounce to this possibility and avoid the calibration of up to four additional free parameters.

Model Application and Evaluation

PREVAH was operated alternating the four snowmelt modules. The model calibration was performed manually.

The basis calibration of the runoff generation module (using the PDDI snowmelt module) was target of an earlier study (Gurtz *et al.* 2003) and included the period 1993-1995. The parameters to be calibrated are the factor controlling the rate of soil moisture recharge through infiltration, the percolation rate (*PERC*) and the storage coefficients which govern the process of runoff generation (K_0 for surface runoff, K_1 for interflow and K_2 for baseflow). The calibration period for the detailed snowmelt simulation was 1982-1985, and included a new adjustment of the storage coefficients for each of the snowmelt modules. The year 1981 was adopted as initialization period and was therefore excluded at the start of the simulation because of the uncertainty of the initial values for the snow water equivalent and for the water storages within the catchment at the initialization of the simulation. The calibration effort differed, depending on the method chosen for the snowmelt computation. A sensitivity test of the parameters controlling the separation between rain and snow was also part of the calibration phase (Pos 2001). Table 2 gives an overview of the calibration of the free parameters within the snowmelt modules. The difference in the calibrated runoff parameters is rather limited (COMB and PDDI have slightly different storage coefficients for the generation of surface runoff and interflow as compared to EMA and ESCIMO). It is therefore expected that the differences in performance found in the four runs are caused in the first instance by the quality of the respective snowmelt modules.

The efficiency coefficient E_2 (Legates and McCabe 1999, Nash and Sutcliffe 1970) is used to evaluate the simulated (S) with respect to the observed hourly discharge (O)

$$E_2 = 1 - \frac{\sum_{i=1}^{n} |O_i - S_i|^2}{\sum_{i=1}^{n} |O_i - [\frac{1}{n} \sum_{i=1}^{n} O_i]|^2} \quad (5)$$

Also the logarithmic formulation of E_2 (Schulla 1997; Hock 1999) was considered. However, it appeared to be not suitable to determine the quality of the snowmelt simulation. The logarithmic efficiency criterion gives valuable indications on the model performance during the low-flow periods in winter, when snowmelt is negligible (Gurtz *et al.* 2003). As further index of model performance the difference between computed and measured yearly discharge is accounted and analyzed. Finally, a graphic comparison between the simulated and the measured hydrographs was made in the calibration phase for a subjective estimation of the simulation performance.

Results

Statistical Performance of the Snowmelt Approaches

Table 3 shows the mean annual simulation results of all four snowmelt approaches. The left hand part of Table 3 only considers the period of the calibration of the snow modules (1982-1985) and of the runoff generation module (1993-1995). The right hand part of Table 3 summarizes the statistical performance in the validation periods (1986-1992 and 1996-2000). Additionally, the mean annual differences between the simulated (S) and the observed (O) discharges are indicated for both periods.

Table 3 – Simulation performances between observed (O) and simulated (S) hourly discharge. Left columns: Calibration period (1982-1985 and 1993-1995). Right columns: validation period (1986-1992 and 1996-2000).

	Calibration Period			Validation Period		
	E_2	S [mm y^{-1}]	$S-O$ [mm y^{-1}]	E_2	S [mm y^{-1}]	$S-O$ [mm y^{-1}]
PDDI	0.867	1328	33	0.880	1205	-12
COMB	0.864	1330	35	0.865	1208	-9
EMA	0.882	1327	32	0.896	1203	-14
ESCIMO	0.862	1330	35	0.840	1193	-24

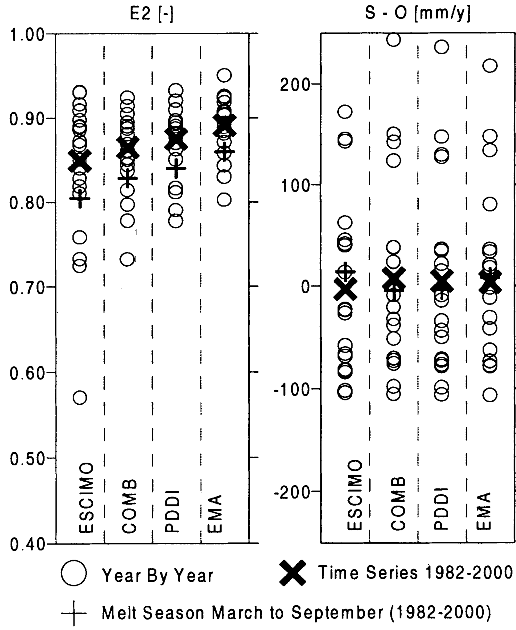

Fig. 2. Variability of the simulation performances. Left: Statistical efficiency. Right: Bias between observed (*O*) and simulated discharges (*S*).

Only ESCIMO shows a slightly worse simulation in the validation period than in the calibration period. To some extent this difference is caused by an outlying point (the year 1992) in the validation period (Fig. 2). The PDDI and the COMB approaches show almost identical efficiencies during the calibration period, however, the more simple PDDI shows slightly better results in the validation period. The EMA performs well in general with an E_2 of 0.891 over the whole period. The sum of the differences between simulated and observed discharge rates is 0.3%. Table 3 exemplifies that the difference between simulation and observation is positive in the calibration period and negative in the validation period. This is also shown in the other three snowmelt modules. The cause of this behavior is not completely understood. A minor correspondence was found between this change of sign in the differences and the mass balance of the Silvretta glacier (Dyurgerov 2002), which is located some 15 kilometers northeast from the Dischma valley. The average mass balance of the Silvretta glacier is -95 mm y^{-1} in the years where PREVAH was calibrated and -420 mm y^{-1} in the validation years. This means that years with limited negative, or positive, mass balance at Silvretta glacier are found more often in the calibration than in the evaluation period. The model might therefore slightly overestimate the runoff rates in years with moderate ice melt and underestimate the runoff rates in years with high ablation rates.

The analysis of the year by year variability of the model efficiency (Fig. 2) brings further indications. The ESCIMO simulation is characterized by a very large difference of efficiency from year to year with E_2 ranging between 0.57 and 0.93 and a standard deviation of 0.09. The other three methods show a reduced range between the years with the highest and the lowest E_2 with standard deviations below 0.05. Evident differences for E_2 are shown in the evaluation of the annual time series and those of the period of March to September. E_2 during the melt season shows higher values in the case of EMA (0.86) and lower values in the case of ESCIMO (0.8).

The average difference between observations and simulations (1982-2000) is smaller than 1.0% for any of the four simulations, which is even lower than the measurement error which is expected to be about 5%. The deviation in the single years can be up to ±10%. ESCIMO shows the smallest standard deviation (87 mm) of the year by year deviation from the observations and a better long term balance between observed and simulated runoff. The COMB and the PDDI runs have the largest range between years with negative and positive difference between observed and simulated discharge (standard deviation above 95 mm, Fig. 2, right). On the other hand Fig. 2 shows that the balance during the snowmelt season is less accurate in the case of ESCIMO, which is a relevant negative aspect of the overall performance of the model. This result indicates the importance of the statistical analysis of the results, not only for the whole period but also for the sub-periods, which are more relevant for the processes under investigation.

Discharge Simulations

Fig. 3 allows some general considerations of the catchment discharge regime. The runoff generation is strongly governed by the processes of snow accumulation and snowmelt. Rainfall shows to have some influence on the discharge regime only between June and October. The mean role of sublimation/evapotranspiration is limited.

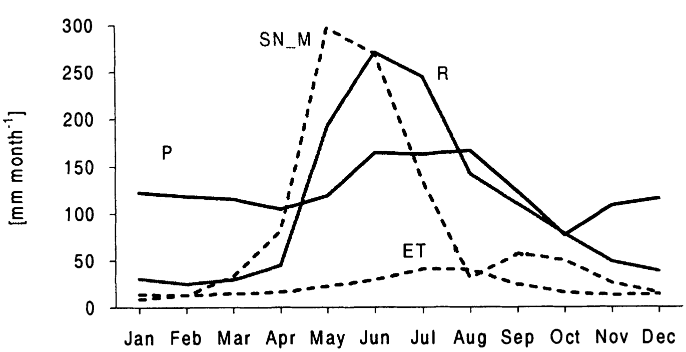

Fig. 3. Average seasonal course (1982-2000) of the main water balance elements simulated with PREVAH and the EMA snowmelt module. *P* is the interpolated precipitation, *R* the discharge, *ET* the sublimation/evapotranspiration and *SN_M* the snow melt.

Table 4 – Simulated water balance (*WB*) over the period 1982-2000. *P* is the interpolated precipitation, *R* the discharge, *ET* the sublimation/evapotranspiration and *SN_M* the snowmelt. *WB* is equal to *P* minus *R* minus *ET*. All units are mm y^{-1}.

Model	*P*	*SN_M*	*ET*	*R*	*WB*
PDDI	1493	1010	258	1251	-16
COMB	1493	1014	256	1253	-17
EMA	1493	1031	254	1249	-11
ESCIMO	1464	977	246	1243	-25

The snowmelt amounts indicate that 60 to 70% of the catchment precipitation occurs as snowfall, thus underlining the importance of the snow model quality for the hydrological simulation in the Dischmabach.

Table 4 indicates that the simulated water balance elements of each of the four PREVAH runs show only limited differences. The different precipitation correction adopted for rain and snow (Sevruk 1986) combined with the different portions of snow and rain computed with Eq. (1) causes the difference between the average precipitation for all model runs using the temperature-index based methods (1,493 mm y^{-1}) and the ESCIMO model run (1,464 mm y^{-1}) This happens because ESCIMO does not consider a temperature range to separate rain and snow (Table 2).

Fig. 4 shows the quality of the simulated discharge regime. All snowmelt methods allow a good reconstruction of the average monthly discharge. The average standard deviation of the monthly runoff rates (given in mm per hour) is also well reproduced. This indicates that the models simulate the discharge variability correctly. However, all the methods used show a too large average standard deviation between January and March, which is an indication for isolated small snowmelt events in late winter and in early spring, which are not confirmed by the observations. This behavior is caused by the strict parameterization of the model, which is constant for the whole catchment throughout the year. A higher threshold temperature T_{GR} at lower elevation zones as compared to higher parts of the catchment would probably eliminate this discrepancy between simulation and observation. In addition, ESCIMO tends to have problems simulating the discharge variability in May, at the onset of the main melt season.

The efficiency analysis, the comparison of the discharge regimes and of the simulated water balance elements indicate that all snow models considered are suitable for snowmelt computation in this alpine catchment. The EMA has a limited requirement for meteorological data, but is able to determine the strong daily cyclicity of the snowmelt. The simple energy balance parameterization of COMB increases its requirements for data and its need for parameter calibration as compared to PDDI and EMA. However, the results show that in the case of the Dischmabach catchment this complexity does not bring any improvement in the discharge simulation. ESCIMO requires a large amount of meteorological data and is based on a strict parame-

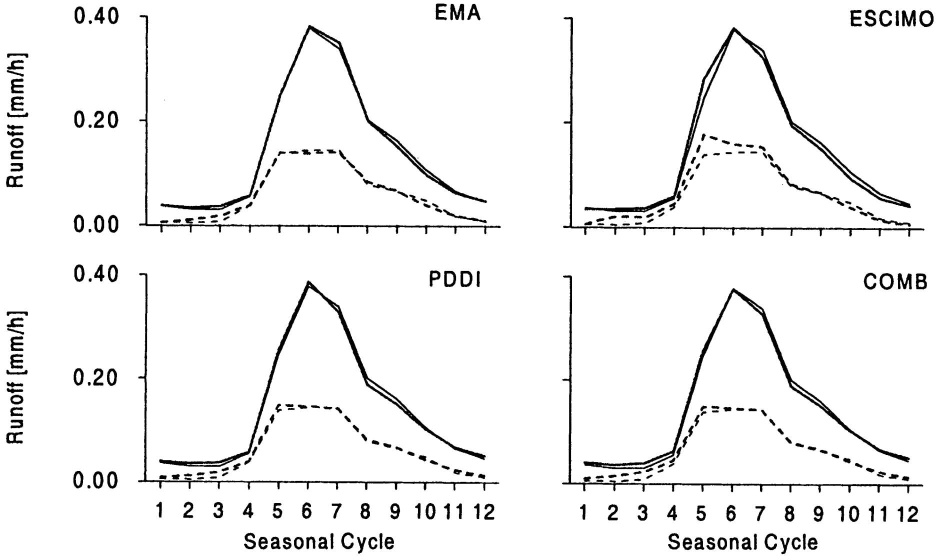

Fig. 4. Observed (thick) and simulated (thin) average monthly discharge (full line, in mm h^{-1}) and the respective average standard deviation (dashed, in mm h^{-1}) from January to December.

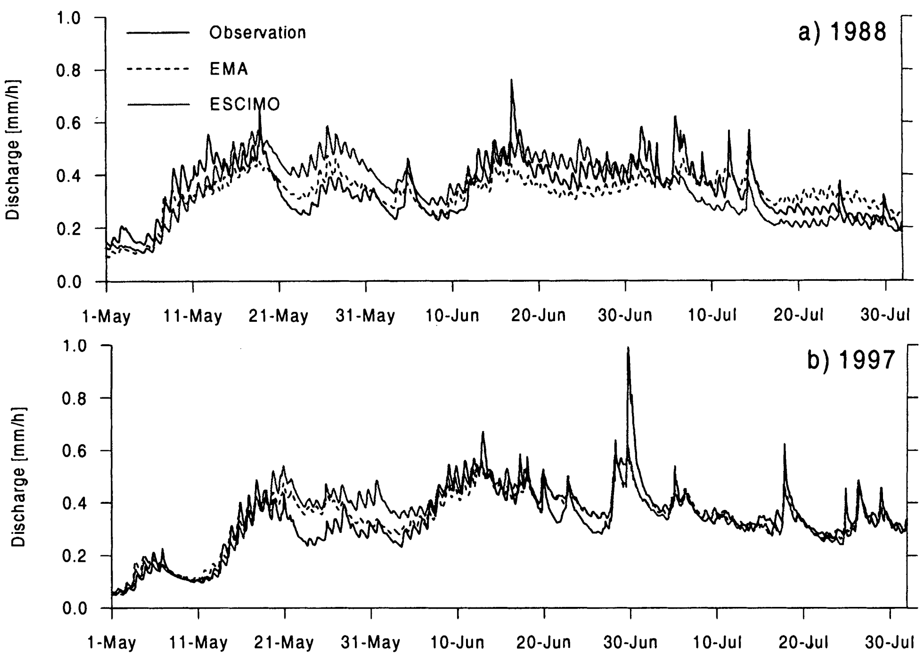

Fig. 5. Hourly runoff hydrograph of Dischmabach between May and July in 1988 (a) and 1997 (b).

terization of the energy balance. This reduces to need for calibration, but in all ESCIMO yields the poorest statistical performance.

Since EMA was the best performing temperature-index based method in the Dischmabach catchment, the remainder of this paper will only discuss the simulation runs using EMA and ESCIMO. It was found that both PPDI and COMB simulate almost identical SWE values as compared to EMA and therefore the evaluation of the SWE simulation with EMA reflects to some extent also the quality of the simulation with the other two temperature-index based methods.

Fig. 5 presents the hourly runoff hydrograph between May and July in 1988 and 1997. The graph shows how the runoff regime is characterized by daily fluctuations, which are reproduced reasonably well by the ESCIMO and EMA simulation. The amplitude of the fluctuations is larger in May, when most of the runoff is generated between 2,100-2,500 m a.s.l., than in July, when the highest snowmelt rates occur above 2,600 m a.s.l. (Figs. 8-10). Both models capture this behavior, which is probably caused by the gradual reduction of water supply by snowmelt due also to a smaller extension of snow covered areas later in the melt season.

ESCIMO shows the tendency to accelerate the course of the snowmelt season (Fig. 5). As also previously observed (Fig. 4) ESCIMO generates too much runoff between May 20 and the June 10 both in 1988 (E_2 May-July = 0.31) and 1997 (E_2 = 0.69) and, especially in 1988, tends to underestimate the runoff later in the melting season.

The EMA shows a better performance than ESCIMO in both 1988 (E_2 May-July = 0.58) and 1997 (E_2 = 0.80). The largest bias is also in case of EMA related to the period of snowmelt onset in the elevations between 2,100 and 2,500 m a.s.l.

Simulation of the Snow Water Equivalent

The Institute for Snow and Avalanche Research (SLF) in Davos measures the snow water equivalent (SWE) at four sites (Fig. 1) in the neighborhood of the Dischmabach catchment the 1st and 15th day of each month between November and July. None of these sites is located within the catchment. Therefore, the observations have been compared to the simulated snow water equivalent of an HRU with similar elevation and aspect as the station under consideration. Only the Stillbergalp station showed to be representative for the evaluation of the results in the Dischma valley. For the stations Flüelastrasse, Büschalp and Weissfluhjoch the simulated SWE is considerably lower than the observations, although the observed and simulated timing of snow accumulation and snowmelt correspond well to ESCIMO and EMA (Pos 2001). These three stations are situated in a neighboring valley with different orientation than the Dischma valley. The different orientation causes a larger amount of precipitation on the slopes to the north-west of Davos (Fig. 1) as compared to the Dischmabach catchment.

Only the Stillbergalp site was therefore suitable for a quantitative comparison with simulated SWE. The simulated SWE (Fig. 6) for deadlines in consecutive 15-

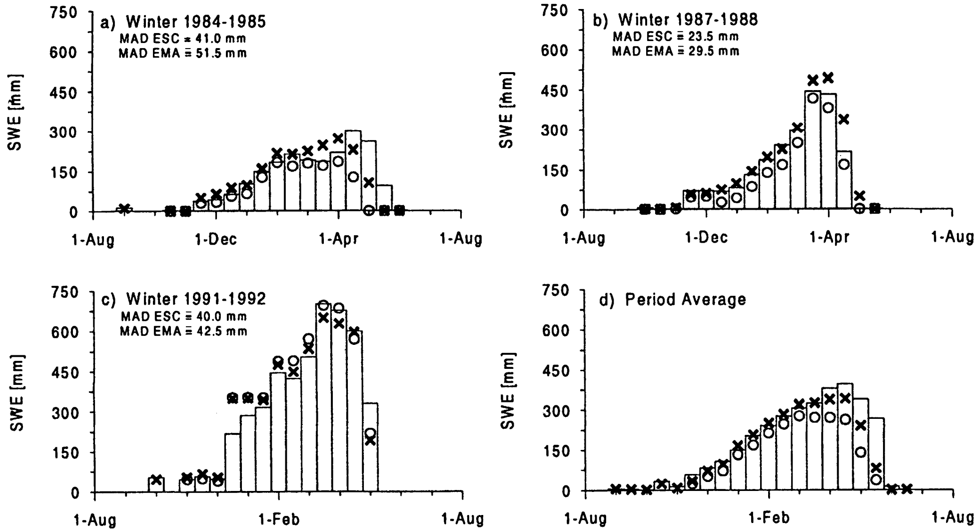

Fig. 6. Stillbergalp (1,970 m a.s.l.): Three winters and the period average (1982-2000) of the observed (bars) and the simulated (symbols) snow water equivalent (SWE) are shown. The crosses identify the ESCIMO simulation, the circles the EMA simulation. The mean absolute deviation (MAD) between simulations and observation during the three winters is also given.

day intervals fits well for the Stillbergalp site, which is located less than one kilometer away from the HRU used for the model evaluation. The average timing of the seasonal course of snow accumulation and melt is fairly good. The SWE simulations with ESCIMO and with the EMA are similar. However, ESCIMO (correlation r^2 = 0.82) fits slightly better in the observed values than EMA (r^2 = 0.79). The two melt models have a similar performance during three winters with different snow conditions, as well as the in case of the 'average winter' (Fig. 6):

a) The winter of 1984-1985 has little snowfall and snow accumulation. Both ESCIMO and EMA reproduce the accumulation phase well, but they terminate the melt season too early.
b) The winter of 1987-1988 was dry until mid-February, when many snowfall events followed until the end of March. EMA underestimates the observed SWE throughout this winter. ESCIMO shows a good agreement with the observations during the whole winter. In both cases the course of snow accumulation and ablation is well captured.
c) The winter of 1991-1992 was characterized by a large accumulation of snow. The two snow models succeed well in the reconstruction of the features of the hydrological processes in this winter with 'extreme' snow conditions.

d) The overall quality of the SWE simulation (winters 1982-2000) is better with respect to the accumulation phase than with respect to the ablation phase. The timing of both phases of the snowpack cycle is simulated very well by both models. However, ESCIMO and, to a larger extent, EMA underestimate the average amount of snow stored during the winter at Stillbergalp and show too high melt rates in May.

In all the three discussed winters the SWE simulated with ESCIMO show a smaller mean absolute deviation (MAD) than SWE determined with EMA with respect to the observed values (Figs. 6a, 6b and 6c). Considering the overall performance, ESCIMO is capable of capturing the local climatological characteristics of Stillbergalp with a higher reliability than EMA. This is due to the fact that in ESCIMO only the snow albedo simulation is controlled by catchment-specific parameters, while in the case of EMA the local features can only be captured by the site adjusted clear-sky direct solar radiation.

Altitudinal Differentiation of Key Hydrological Processes

Fig. 7 shows the average monthly spatially interpolated 2 metres air temperature and precipitation at different elevation zones. Fig. 8 shows the computed contribution of the different elevation zones to the catchment snowmelt for the months of April to July. In April the total catchment melt originates from levels between 1,600-2,000 m a.s.l. where the average air temperature is above the 0° isotherm. In May the elevation range with maximum snowmelt shifts to 2,100-2,500 m a.s.l., where the largest part of the catchment is located (right hand plot in Fig. 8). This explains the increase in runoff between the 1st and 31st of May (Fig. 5). The runoff maximum in the Dischmabach is caused by a superposition of the main snowmelt season in the area between 2,100-2,800 m a.s.l. and the period with maximum rainfall (Fig. 7 and Fig. 3).

Fig. 9 presents the altitudinal dependence of the snowmelt in the months of April to June as simulated with EMA (each symbol represents a HRU and its aspect). In April the south and west exposed HRUs between 1,900 and 2,400 m a.s.l show larger average snowmelt rates than the north and west exposed areas. In May the average snowmelt occurs between 1,900 and 2,400 m a.s.l., mainly in the north and east exposed HRUs. Above 2,400 m a.s.l. the west and south exposed HRUs show higher snowmelt than north and east exposed HRUs. This behavior is caused by the different amounts of energy available for the melting processes with respect to elevation and aspect. This process is well-understood for north and south-exposed HRUs, but is worth further discussion in the case of the east and west exposed HRUs, which theoretically get the same amount of potential radiation. The differences are a result of the temporal shift between the radiation input in the east and west-oriented slopes. East-oriented slopes already dispose of direct solar radiation early in the morning (maximum at approximately 10 a.m.), when the surface air temperature is often below melting point. West-exposed areas receive direct radiation later (maximum in-

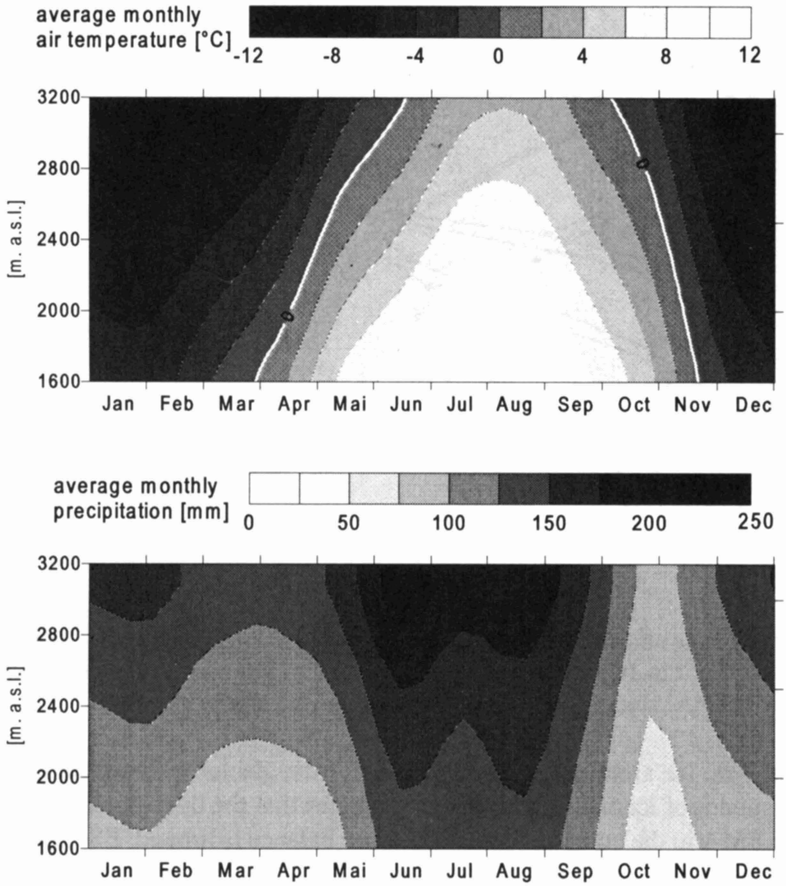

Fig. 7. Dischmabach, 1982-2000: Monthly averages of 2 metres air temperature and precipitation at the different 100 m elevation zones.

come at about 15 p.m.), when the air temperature is more often above melting point. These differences are hydrologically relevant when the daily air temperature cycle fluctuates around the melting point. The ESCIMO run demonstrated a similar response to elevation and exposure.

Fig. 10a illustrates the altitudinal dependence of the average monthly water balance in the case of the EMA method. The period with a positive water balance (increase of water storage) differs considerably with respect to the elevation and is governed by both the snowmelt season, the annual course of precipitation (Fig. 7) and surface air temperature (Fig. 7). At 1,700 m a.s.l, the water balance is negative (release of water) in March, while above 3,000 m a.s.l. this happens after May. This demonstrates the temporal shift of the snowmelt season onset with respect to the elevation. The large negative balance at 2,800 m a.s.l. in July and August is due to the

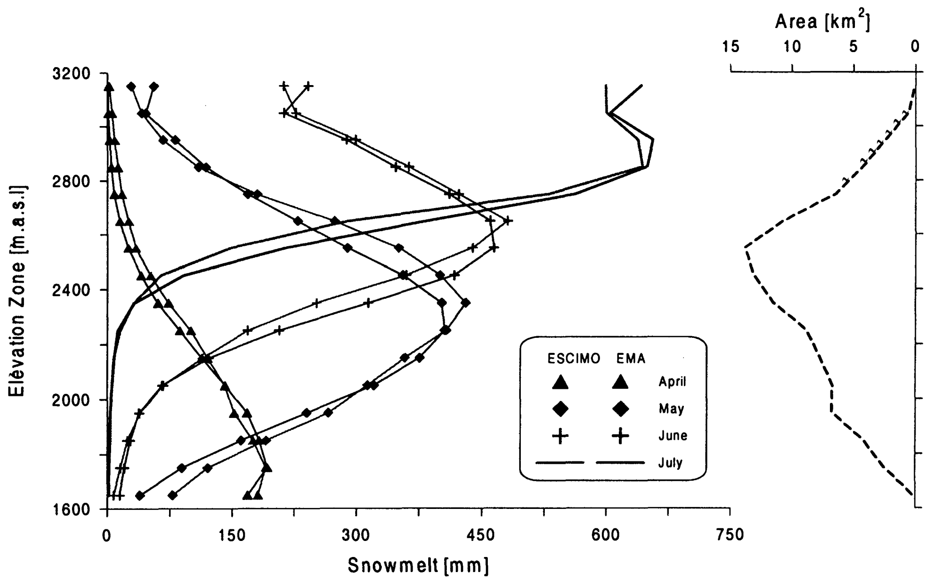

Fig. 8. Left: Average altitudinal distribution of the simulated snowmelt (1982-2000) for the months April to July determined using ESCIMO (gray) and the extended melt approach (EMA, black). Right: Catchment area at each elevation zone.

presence of bare ice areas in the ablation zone of the glacier which generate a considerable amount of icemelt. Fig. 10b demonstrates that the difference between ESCIMO and EMA in the computed monthly water balance is limited. ESCIMO shows a more negative water balance in May below 2,700 m a.s.l. and in August above 3,000 m a.s.l. Above 2,400 m a.s.l. the water balance of July is more negative in the case of EMA. This indicates that in case of EMA the ablation zone of the glacier is clear of snow earlier than for ESCIMO and that therefore higher icemelt rates are computed.

Fig. 9. Monthly snowmelt of the HRUs with respect to elevation and exposure (symbols). HRUs representing water surfaces are not plotted, since snow accumulation is not allowed for such HRUs. The data are based on the simulation with the extended melt approach over the period 1982-2000.

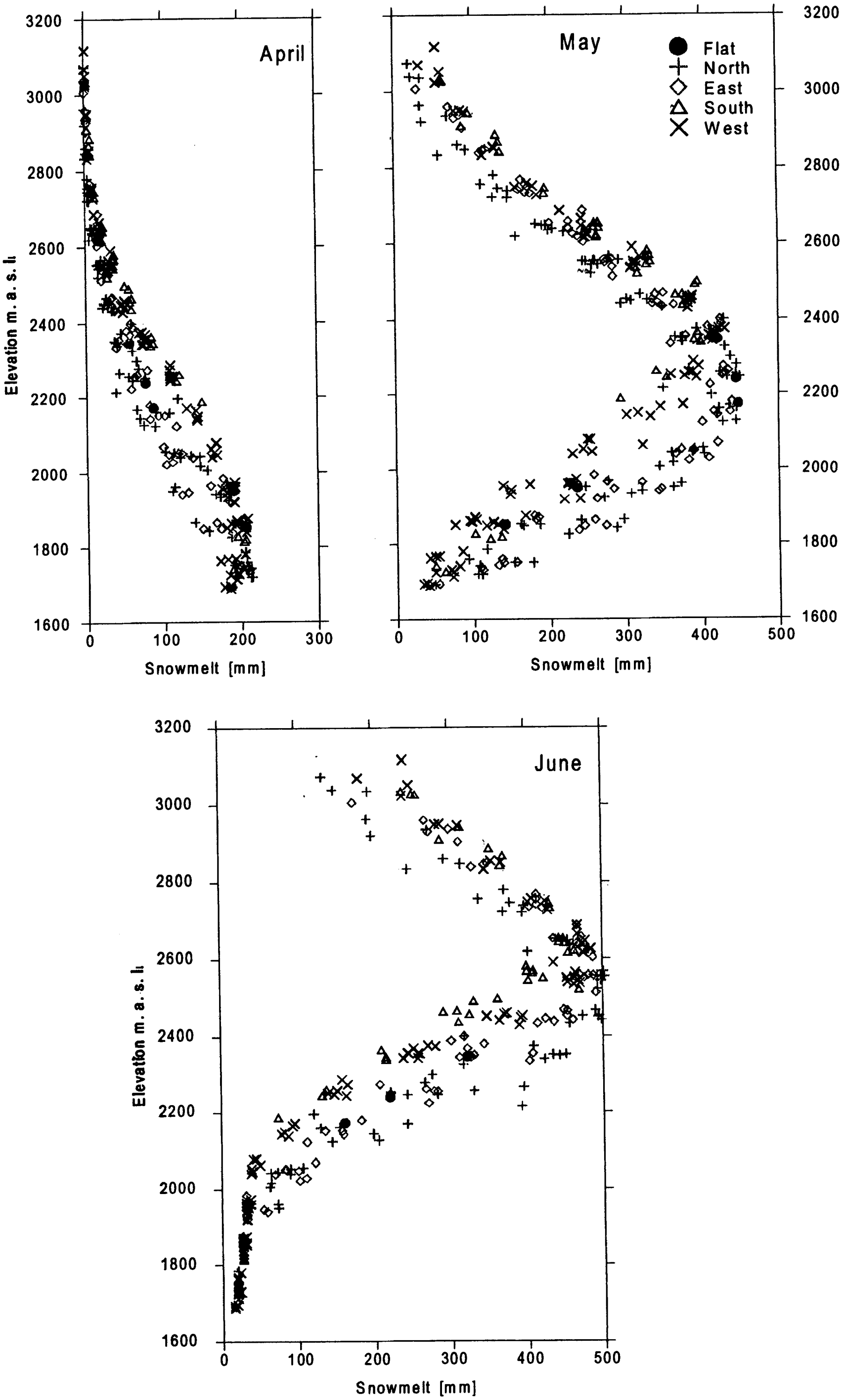
April
May
June
Flat
North
East
South
West
Elevation m. a. s. l.
Snowmelt [mm]
3200
3000
2800
2600
2400
2200
2000
1800
1600
0
100
200
300
400
500

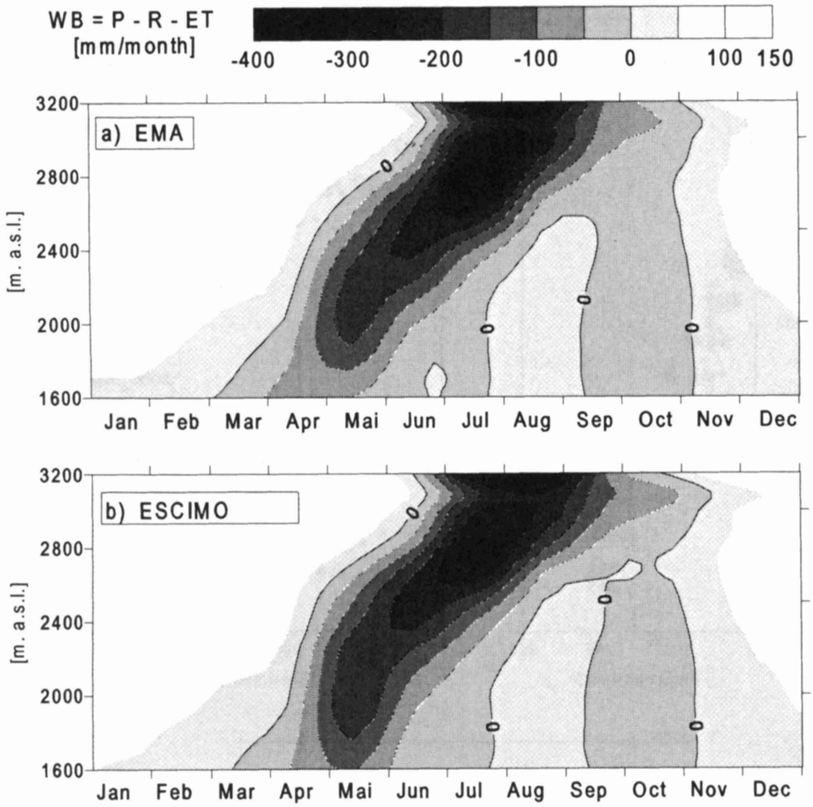

Fig. 10. Dischmabach, seasonal water balance, 1982-2000: The water balance at each elevation zone (*WB*) was computed subtracting the simulated runoff (*R*) and the simulated evapotranspiration (*ET*) from the interpolated precipitation (*P*). (a) average simulated monthly water balance with respect to elevation determined by using the extended melt approach (EMA). (b): as a) using ESCIMO.

Summary and Conclusions

This study confirms the importance of the snowmelt module for a sound spatially distributed modelling of the hydrological cycle in alpine catchments. A working snowmelt module can be simple, due to the implicit relevance of air temperature in the surface layer for the computation of the seasonal course of snowpack. Four methods for the spatially distributed simulation of snow hydrology at catchment scale have been compared. All of them appear to be suitable to compute the runoff hydrograph of an alpine catchment with runoff regime governed by snowmelt. This is confirmed by the year-to-year analysis of the model efficiency as well as by the analysis of the water balance. The quality of the results obtained from the calibration and validation is similar.

The three temperature-index based methods showed to a great extent similar efficiencies, however, the inclusion of the potential clear-sky radiation appears to be an evident improvement in the reconstruction of the daily runoff hydrograph fluctuations without the need of additional observations with respect to the classic PDDI approach (Table 2). Since the potential clear-sky radiation is subject to high spatial and temporal variations, it can be concluded that the improved efficiency is due to the important role played by topography for the spatial and temporal distribution of snowmelt (and runoff) generation. If the interest is limited to daily or monthly discharges, then all of the temperature-index based methods are suitable. In lowland regions where such daily fluctuations of the discharge rates are smaller and rain-on-snow events more frequent it is probably less evident that EMA is superior to both PDDI and COMB.

The simulation based on ESCIMO is characterized by a very large variation in quality from year to year. This variability is better captured by the temperature-index methods. The physically based structure of ESCIMO is more sensitive to the quality of the meteorological input than the conceptual structure of temperature-index based approaches, since the latter allow the calibration of more free parameters. During the transition period, when the temperature of the snowpack is close to melting condition, considerable errors in the (ESCIMO) simulation of melt rates can occur even due to comparably small uncertainties in the meteorological variables: mainly the phase of the precipitation, rain or snow, has a significant consequence on the energy balance. In this respect the fix threshold temperature for the distinction between rain and snow and that melting conditions occur only at isothermal state of the entire snowpack at 273.16 K can be shortcomings of ESCIMO. Nevertheless, the model structure can not account for the uncertainties of the input data.

The simulation of snow water equivalent was more successful with ESCIMO, since an energy balance based model considers better the local characteristics of the specific catchment unit (grid cell or HRU). The application of ESCIMO instead of a temperature-index based model causes a 20-30% increase in the computational time. However, this increase in computational time is not supported by an increase in quality of the hydrological simulations.

The topographical structure, the seasonal air temperature gradient and the seasonal distribution of precipitation are the main factors which control the discharge hydrograph. The period after the 0° C air temperature isotherm passes the elevation zones with the largest parts of the catchment area is the condition for the highest runoff rates. The level of the runoff maximum is additionally increased if the seasonal precipitation maximum coincides with the snowmelt period in the largest part of the catchment, as was the case in the investigated Dischmabach catchment. The analysis of the seasonal altitudinal distribution of the water balance is of great interest to the management of water resources in alpine catchments such as the optimization of the production of electricity with hydropower or for the planning of new hydropower plants. The results show that PREVAH is a suitable tool to cope with such questions.

Acknowledgements

We thank MeteoSwiss for giving us the access to the meteorological data and the SLF Davos for providing us with the snow water equivalent data. Thanks to four fellow scientists and to the reviewers for their helpful comments to the manuscript.

References

Abbott, M. B., Bathurst, J. C., Cunge, J. A., O'Connell, P. E., and Rasmussen, J. (1986) An Introduction to the European Hydrological System – Système Hydrologique Européen, 'SHE', *J. Hydrol.*, *Vol. 87*, pp. 45-77.

Anderson, E. A. (1973) National Weather Service River Forecast System – Snow Accumulation and Ablation Model. NOAA Tech. Memo. NWS. U.S. Dep. of Commerce, Silver Spring.

Bergström, S. (1976) Development and Application of a Conceptual Runoff Model for Scandinavian Catchments, Bulletin Series A, No. 52, University of Lund.

Beven, K. J. (1989) Changing Ideas in Hydrology – The Case of Physically-Based Models, *J. Hydrol.*, *Vol. 105*, pp. 157-172.

BFLT (1991) Digitales Höhenmodel RIMINI. Bundesamt für Landestopographie, Wabern, Switzerland.

BFS (1995) Die Bodennutzung der Schweiz. Arealstatistik 1979/85. Bundesamt für Statistik, Bern, Switzerland.

Blöschl, G., and Sivapalan, M. (1995) Scale Issues in Hydrological Modelling – a Review, *Hydrol. Process.*, *Vol. 9*, pp. 251-290.

Blöschl, G. (1999) Scaling Issues in Snow Hydrology, *Hydrol. Process.*, *Vol. 13*, pp. 2149-2175.

Braun, L. (1985) Simulation of Snowmelt-Runoff in Lowland and Lower Alpine Regions of Switzerland, *Zuer. Geogr. Schriften*, Heft 21.

Braun, L., Brun, E., Durand, Y., and Martin, E. (1994) Simulation of Discharge using Different Methods of Meteorological Data Distribution, Basin Discretization and Snow Modelling, *Nord. Hydrol.*, *Vol. 25*, pp. 129-144.

Dyurgerov, M. (2002) *Glacier Mass Balance and Regime: Data of Measurements and Analysis*, Occasional Paper No. 55, Institute of Arctic and Alpine Research, University of Colorado.

Essery, R., Martin, E., Douville, H., Fernandez, A., and Brun, E. (1999) A comparison of four snow models using observations from an alpine site, *Clim. Dyn.*, *Vol. 15*, pp. 583-593.

Ferguson, R. I. (1999) Snowmelt Runoff Models, *Progress In Physical Geography*, *Vol. 23 (2)*, pp. 205-227.

Gurtz, J., Baltensweiler, A., and Lang, H. (1999) Spatially distributed hydrotope-based modelling of evapotranspiration and runoff in mountainous basins, *Hydrol. Process., Vol. 13*, pp. 2751-2768.

Gurtz, J., Zappa, M., Jasper, K., Lang, H., Verbunt, M., Badoux, A., and Vitvar, T. (2003) A Comparative Study in Modelling Runoff and its Components in Two Mountainous Catchments. *Hydrol. Process. Vol. 17*, pp. 297-311.

Hock, R. (2003) Evaluation and recent developments in temperature-index melt modelling in mountain regions. *J. Hydrol. in print.*

Hock, R. (1999) Distributed temperature-index ice- and snowmelt model including potential direct solar radiation, *J. Glaciol., Vol. 45* (149), pp. 101-111.

Kirnbauer, R., Blöschl, G., and Gutknecht, D. (1994) Entering the Era of Distributed Snow Models, *Nord. Hydrol., Vol. 25*, pp. 1-24.

Klemes, V. (1990) The Modelling of Mountain Hydrology: the Ultimate Challenge, *Hydrology of Mountainous Areas*, L. Molar, Ed. *IAHS, Vol. 190*, pp. 29-43.

Klok, E. J., Jasper, K., Roelofsma, K. P., Badoux, A., and Gurtz, J. (2001) Distributed hydrological modelling of a glaciated Alpine river basin, *Hydrol. Sci. J., Vol. 46*, pp. 553-570.

Lang, H., and Braun, L. (1990) On the Information content of air Temperature in the Context of Snow Melt Estimation, *Hydrology of Mountainous Areas*, L. Molar, Ed. *IAHS, Vol. 190*, pp. 347-354.

Legates, D. R., and McCabe, G. J. (1999) Evaluating the Use of "Goodness-of-Fit" measures in hydrologic and hydroclimatic model validation, *Water Resour. Res., Vol. 35*, pp. 233-241.

Monteith, J. L. (1965) Evaporation and Environment, *Symp. Soc. Exp. Biol., Vol. 19*, pp. 205-234.

Nash, J. E., and Sutcliffe, J. V. (1970) River flow forecasting through conceptual models (1), a discussion of principles, *J. Hydrol., Vol. 10* (3), pp. 282-290.

Ohmura, A. (2001) Physical Basis for the Temperature-Based Melt-Index Method, *J. Appl. Meteor.*, Vol. 40, pp. 753-761.

Pos, F. (2001) Spatially distributed modelling of snow accumulation and melt in pre-alpine and alpine catchments. Diploma Thesis, Wageningen University.

Rohrer, M.B. , Braun, L. N., and Lang, H. (1994) Long Term Records of Snow Cover Water Equivalent in The Swiss Alps: 2. Simulation, *Nord. Hydr*ol., *Vol. 25*, pp. 67-78.

Schulla, J. (1997) Hydrologische Modellierung von Flussgebieten zur Abschätzung der Folgen von Klimaänderungen, *Zuer. Geogr. Schriften,* Heft 69.

Sevruk, B. (ed.) (1986) Correction of Precipitation Measurements. ETH/IASH/WMO Workshop on the Correction of Precipitation Measurements. Zürich, April 1-3, 1985, *Zuer. Geogr. Schriften,* Heft 23.

Slater, A. G., Schlosser, C. A., Desborough, C. E., Pitman, A. J., Henderson-Sellers, A., Robock, A., Vinnikov, K. Ya., Mitchell, K., and the PILPS 2(d) Contributors (2001): The Representation of Snow in Land-surface Schemes; Results from PILPS 2(d), *J. Hydrometeorology, Vol. 2*, pp. 7-25

Strasser, U., and Mauser, W. (2001) Modelling the Spatial and Temporal Variations of the Water Balance for the Weser Catchment 1965-1994, *J. Hydrol., Vol. 254*, pp. 199-214.

Strasser, U., Etchevers, P., and Lejeune, Y. (2001) Modelling the Seasonal Snow Cover with CROCUS and ESCIMO Using Data from the Col de Porte Station. In: Note du Travail du Centre d'Etudes de la Neige, *Vol. 16*, pp. 1-15, Meteo-France, Paris.

WMO (1986) Intercomparison of models of snowmelt runoff. Operational Hydrology Report 23, World Meteorological Organization, Geneva.

Zappa, M., Badoux, A., and Gurtz, J. (2000) The application of a complex distributed hydrological model in an highly glaciated alpine river catchment, in *Limnological Reports*, Horvatic, J. (Editor), 33rd Conference of International Association for Danube Research, Osijek, Croatia, 3-9 September 2000, *Vol. 33*, pp. 23-28.

Received: 9 April, 2002
Revised: 21 June, 2002
Accepted: 23 July, 2002

Addresses:
Massimiliano Zappa,
Institute for Atmospheric and Climate Science,
Winterthurerstrasse 190,
CH-8057 Zürich,
Switzerland.
Email: zappa@iac.umnw.ethz.ch

J. Gurtz same address

F. Pos and P. Warmerdam,
Department of Environmental Sciences,
Wageningen University

U. Strasser,
Inst. of Hydromechanics and
Water Resources Management,
ETH, Zürich.